4、 外语能力证书

RSC Advances

PAPER

View Article Online
View Journal | View Issue

Cite this: *RSC Adv.*, 2024, **14**, 6085

Design, synthesis, and inhibitory activity of hydroquinone ester derivatives against mushroom tyrosinase†

Dong Xie,‡[a] Kangjia Han,‡[a] Qian Jiang,[a] Sida Xie,[a] Jielong Zhou,[a] Yingjun Zhang,[b] Junming Xu,[c] Yuanping He,[d] Ping Zhao*[e] and Xiaoqin Yang*[a]

Tyrosinase is a widely distributed copper-containing enzyme found in various organisms, playing a crucial role in the process of melanin production. Inhibiting its activity can reduce skin pigmentation. Hydroquinone is an efficient inhibitor of tyrosinase, but its safety has been a subject of debate. In this research, a scaffold hybridization strategy was employed to synthesize a series of hydroquinone–benzoyl ester analogs (**3a–3g**). The synthesized compounds were evaluated for their inhibitory activity against mushroom tyrosinase (mTyr). The results revealed that these hydroquinone–benzoyl ester analogs exhibited inhibitory activity against mTyr, with compounds **3a–3e** displaying higher activity, with compound **3b** demonstrating the highest potency ($IC_{50} = 0.18 \pm 0.06$ μM). Kinetic studies demonstrated that the inhibition of mTyr by compounds **3a–3e** was reversible, although their inhibition mechanisms varied. Compounds **3a** and **3c** exhibited non-competitive inhibition, while **3b** displayed mixed inhibition, and **3d** and **3e** showed competitive inhibition. UV spectroscopy analysis indicated that none of these compounds chelated with copper ions in the active center of the enzyme. Molecular docking simulations and molecular dynamics studies revealed that compounds **3a–3e** could access the active pocket of mTyr and interact with amino acid residues in the active site. These interactions influenced the conformational flexibility of the receptor protein, subsequently affecting substrate–enzyme binding and reducing enzyme catalytic activity, in line with experimental findings. Furthermore, *in vitro* melanoma cytotoxicity assay of compound **3b** demonstrated its higher toxicity to A375 cells, while displaying low toxicity to HaCaT cells, with a dose-dependent effect. These results provide a theoretical foundation and practical basis for the development of novel tyrosinase inhibitors.

Received 1st January 2024
Accepted 5th February 2024

DOI: 10.1039/d4ra00007b

rsc.li/rsc-advances

Introduction

Tyrosinase (EC 1.14.18.1) is a crucial and rate-limiting enzyme responsible for catalyzing melanin synthesis. It is widely distributed in living organisms and intricately linked to numerous pivotal physiological processes. Tyrosinase possesses a complex structure with an active site containing a binuclear copper center situated within the active region. In the presence of oxygen, it efficiently catalyzes the oxidation of phenolic compounds.[1] In mammals, tyrosinase is predominantly located in melanocytes, playing a pivotal role throughout the melanin formation process. Disorders in tyrosinase metabolism within

[a]*Key Laboratory of National Forestry and Grassland Administration on Highly-Efficient Utilization of Forestry Biomass Resources in Southwest China, Southwest Forestry University, Kunming, Yunnan 650224, PR China. E-mail: yangxiaoqin@swfu.edu.cn*

[b]*Laboratory of Phytochemistry and Plant Resources in West China, Kunming Institute of Botany, Chinese Academy of Sciences, Kunming, Yunnan 650204, PR China*

[c]*Institute of Chemical Industry of Forest Products, Chinese Academy of Forestry, Nanjing, Jiangsu 210042, PR China*

[d]*Kunming Beiye Dai Medicine Research Institute, Kunming, Yunnan 650499, PR China*

[e]*Key Laboratory of Ministry of Education for Forest Resources Conservation and Utilization in the Southwest Mountains of China, Southwest Forestry University, Kunming, Yunnan 650224, PR China. E-mail: hypzhao2022@163.com*

† Electronic supplementary information (ESI) available: Fig. S1. ^{1}H NMR and ^{13}C NMR for compound **3a–3g**. Fig. S2. HRMS for compound **3a–3g**. Fig. S3. The inhibitory activity of compound **3a–3g** on mTyr. Fig. S4. Inhibition reversibility (A) and inhibition type (B) of compound **3a**, **3c–3e** on mTyr. Fig. S5. UV Spectra of compound **3a**, **3c–3e** before and after interaction with mTyr. Fig. S6. The crystal structure of mTyr (PDB ID: 2Y9X). Fig. S7. Docking model for compound **3a**, **3c–3e** with mTyr (A) and molecular dynamics results of compound **3a**, **3c–3e** and (**3a**, **3c–3e**)–mTyr complex with: (B) RMSD, (C) RMSF, (D) R_g, (E) SASA, and (F) H-bonds. Table S1. Linear fitting equation, Michaelis constant (K_m), maximum reaction rate (V_m), and inhibition type for mTyr at varying concentrations of compounds **3a–3e**. Table S2. Docking energy and bonding condition of compounds **3a–3e** with mTyr. See DOI: https://doi.org/10.1039/d4ra00007b

‡ Co-first authors. These authors contributed equally to this work.

5、 学术能力证明材料

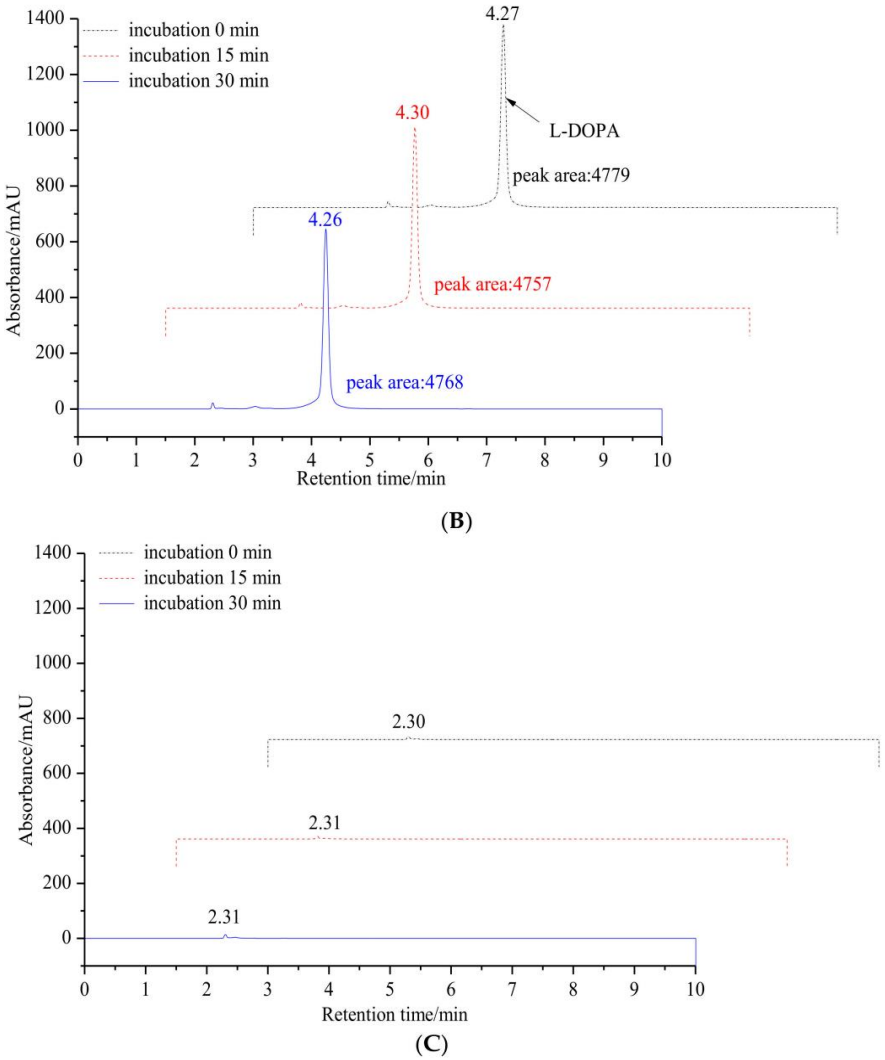

Figure 2. Monitoring changes in the content of L-DOPA oxidation products through HPLC analysis: (**A**). Incubation of L-DOPA as a diphenolase substrate for mTyr without 6′-*O*-caffeoylarbutin at 30 °C with incubation times of 0, 15, and 30 min. (**B**). Incubation of L-DOPA as a diphenolase substrate for mTyr in presence of 6′-*O*-caffeoylarbutin at 30 °C with incubation times of 0, 15, and 30 min. (**C**). Incubation of mTyr in the presence of 6′-*O*-caffeoylarbutin at 30 °C with incubation times of 0, 15, and 30 min at 30 °C.

2.1.2. mTyr Inhibition Kinetics of 6′-*O*-Caffeoylarbutin

Enzyme inhibition can be categorized into two main types, namely reversible and irreversible. To determine the nature of inhibition, the relative reaction rates of enzyme-catalyzed reactions at different inhibitor concentrations can be plotted. Figure 3A illustrates a set of straight lines intersecting at the origin when plotting the relative reaction rate against enzyme concentration under various concentrations of 6′-*O*-caffeoylarbutin. The figure clearly shows that, as the concentration of 6′-*O*-caffeoylarbutin increases, the slope of the lines gradually decreases and eventually intersects at the origin. This indicates that

the inhibitory effect of 6′-*O*-caffeoylarbutin on mTyr is a reversible process, and it does not decrease the total amount of mTyr but rather inhibits its catalytic activity.

Continuing from the Lineweaver_Burk analysis, the inhibition type of 6′-*O*-caffeoylarbutin on mTyr was determined. The inhibition types include competitive inhibition, non-competitive inhibition, uncompetitive inhibition, and mixed-type inhibition, which can be determined by plotting the reciprocal of enzyme reaction rate [1/V] against the reciprocal of substrate concentration [1/S] at different inhibitor concentrations. As shown in Figure 3B, with increasing concentrations of 6′-*O*-caffeoylarbutin, the slope of the straight lines gradually increased, and, ultimately, the double reciprocal curves of enzyme reaction rate and substrate concentration intersected on the y-axis. This indicates that 6′-*O*-caffeoylarbutin inhibits mTyr through competitive inhibition. In other words, 6′-*O*-caffeoylarbutin can bind to the free tyrosinase, competing with the substrate L-DOPA for the binding site of enzyme, thereby inhibiting melanin production. The inhibition constant (Ki) for the binding of the inhibitor to the free enzyme can be calculated from the slope of the double reciprocal curves of different inhibitor concentrations against concentration. The Ki of 6′-*O*-caffeoylarbutin on mTyr was determined to be 1.34 ± 0.92 μM indicating that 6′-*O*-caffeoylarbutin affects the activity of mTyr by binding to the free enzyme, and it likely interacts with only one or a specific class of binding sites [17].

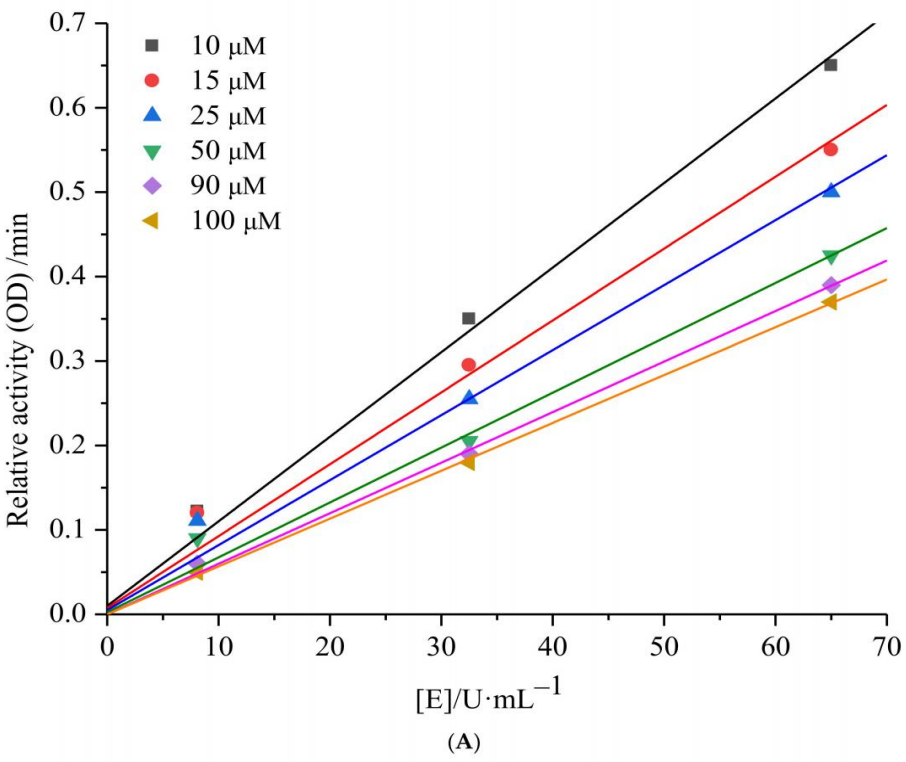

Figure 3. *Cont.*

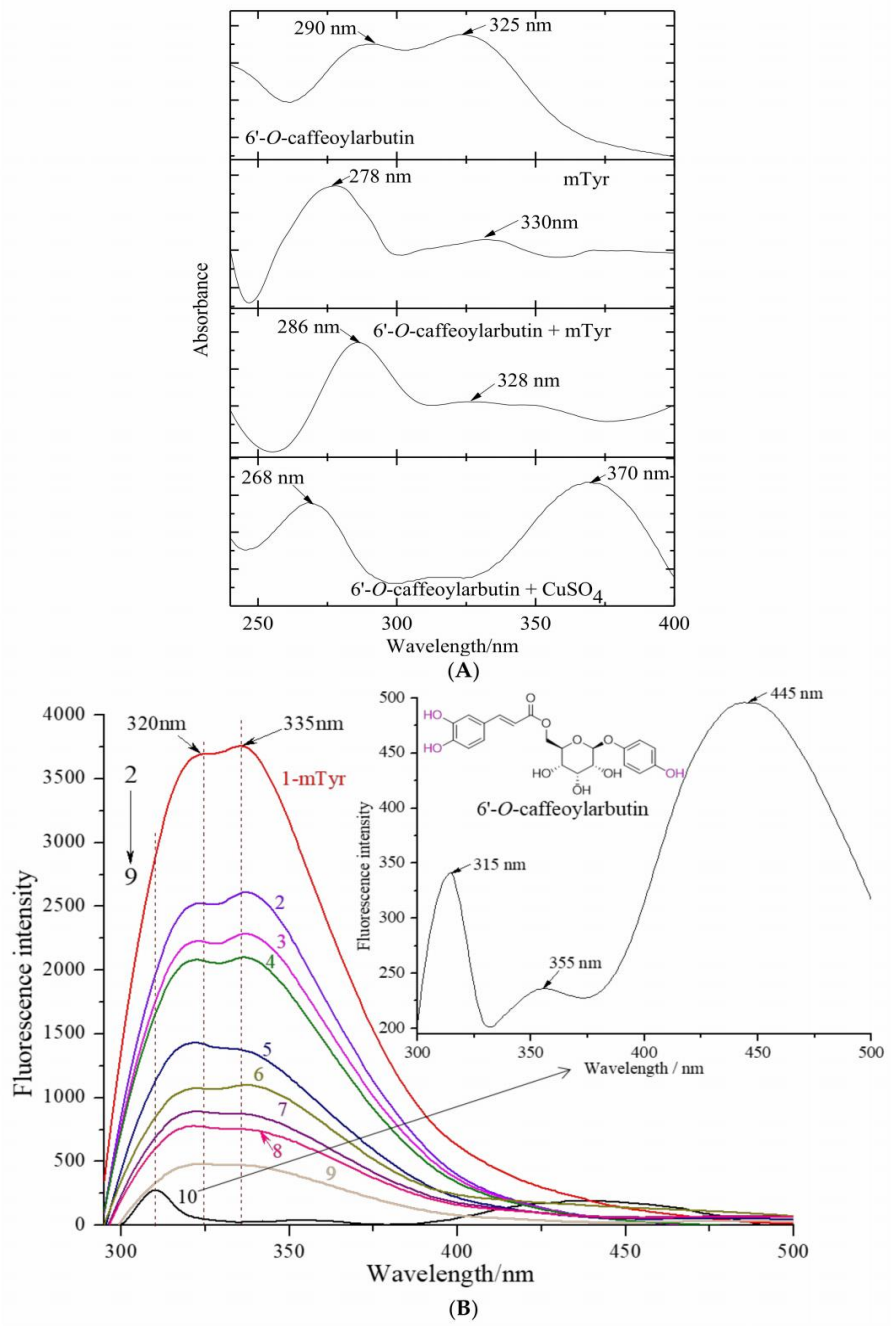

Figure 4. UV_vis spectra for the chelation of 6′-*O*-caffeoylarbutin with copper (II) ion in mTyr and fluorescence quenching effect of 6′-*O*-caffeoylarbutin on mTyr: (**A**). UV_vis spectra for the chelation between 6′-*O*-caffeoylarbutin and copper (II) ions. (**B**). Intrinsic fluorescence spectra of mTyr in the presence of 6′-*O*-caffeoylarbutin at different concentrations; the concentrations of 6′-*O*-caffeoylarbutin for curves 1–9 were 0, 5, 10, 15, 25, 50, 75, 90, and 100 μM, respectively; curve 10 represents the fluorescence intensity of 6′-*O*-caffeoylarbutin at the concentration of 0.02 μM.

2. Results and Discussion

2.1. mTyr Inhibition Mechanism of 6′-O-Caffeoylarbutin

2.1.1. Inhibitory Effect of 6′-*O*-Caffeoylarbutin on Oxidation of L-DOPA Catalyzed by mTyr

6′-*O*-caffeoylarbutin has garnered significant attention due to its abundant presence in Quezui tea and its remarkable anti-melanin activity. Previous research has demonstrated that 6′-*O*-caffeoylarbutin exhibits superior anti-melanin activity compared to the commercial whitening agent beta-arbutin, with the effects of melanin production being fully restored upon removal of 6′-*O*-caffeoylarbutin. As shown in Figure S2, structural analysis reveals that 6′-*O*-caffeoylarbutin is derived from the beta-arbutin structure by adding the caffeic acid moiety with two hydroxyl groups. This modification endows 6′-*O*-caffeoylarbutin with both monophenol and diphenol functionalities. Both beta-arbutin and 6′-*O*-caffeoylarbutin were characterized using NMR (^{1}H and ^{13}C) and spectroscopic data can be found in the Supplementary Material (Figures S3 and S4). Based on these findings, we hypothesized that 6′-*O*-caffeoylarbutin shares a similar mechanism of melanin inhibition with beta-arbutin, which inhibits melanin formation by suppressing the activity of tyrosinase. The enhanced anti-melanin activity of 6′-*O*-caffeoylarbutin can be attributed to its diphenol structure. Furthermore, our previous experiments confirmed that 6′-*O*-caffeoylarbutin effectively inhibits both the monophenolase and diphenolase activities of mTyr, with IC_{50} values of 1.114 ± 0.035 μM and 95.198 ± 1.117 μM, respectively. In comparison, beta-arbutin selectively inhibits the monophenolase activity of mTyr with an IC_{50} of 8.4 mM, while having no inhibitory effect on the diphenolase activity. Notably, 6′-*O*-caffeoylarbutin exhibits stronger inhibition of the diphenolase activity of mTyr compared to the positive control kojic acid (Table S1) [15,16].

To further validate our hypothesis, the inhibitory effect of 6′-*O*-caffeoylarbutin on the diphenolase activity of mTyr was measured by analyzing the oxidation of L-DOPA to DOPA quinones using HPLC. As shown in Figure 2, the oxidation products of L-DOPA significantly decrease with the addition of 6′-*O*-caffeoylarbutin, indicating the suppression of enzyme activity. However, the products do not disappear completely, suggesting that the enzyme activity is not completely inhibited. Therefore, 6′-*O*-caffeoylarbutin is a better inhibitor of mTyr compared to beta-arbutin and kojic acid, and its stronger inhibitory effect on the diphenolase activity of the enzyme may be the main reason for its approximately two-fold higher anti-melanin activity compared to beta-arbutin.

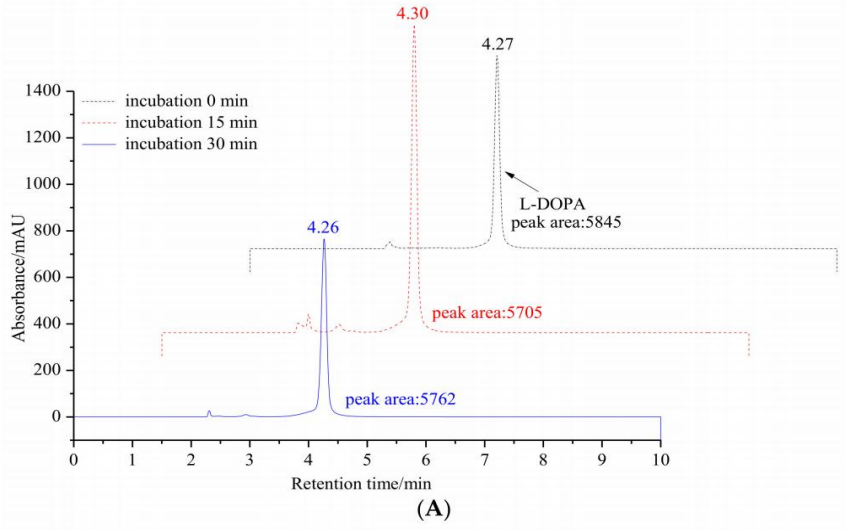

Figure 2. *Cont.*

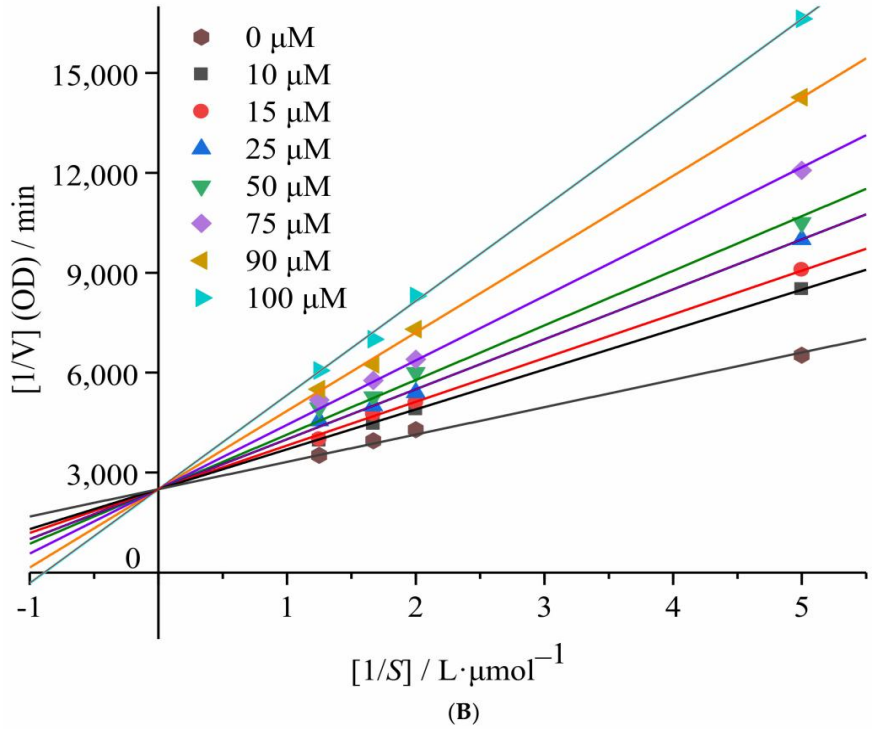

Figure 3. mTyr inhibition kinetics of 6′-*O*-caffeoylarbutin: (**A**). Inhibitory type of 6′-*O*-caffeoylarbutin on mTyr. (**B**). Lineweaver_Burk plots of 6′-*O*-caffeoylarbutin on mTyr.

2.1.3. The Chelation of 6′-*O*-Caffeoylarbutin with Copper (II) Ion in mTyr

mTyr is a binuclear copper-containing glycoenzyme that exhibits two distinct catalytic activities. The active center of mTyr is occupied by copper (II) ions, which play a crucial role in the catalytic cycles by interacting with substrates (Figure 4A). Investigating the interaction between small molecular inhibitors and copper (II) ions can be achieved through significant blue or red shifts in the characteristic absorption bands, making UV_vis spectrometry a valuable tool for studying conformational changes in proteins within enzyme_inhibitor complexes.

Figure 4A presents the UV_vis absorption spectra of a solution containing 6′-*O*-caffeoylarbutin in the presence of mTyr and $CuSO_4$ separately. 6′-*O*-caffeoylarbutin exhibits two characteristic absorption bands: band I at 323 nm, corresponding to n→π* transitions within the acyl group, and band II at 291 nm, corresponding to π→π* transitions within the aromatic group. Upon the addition of copper (II) ion to the 6′-*O*-caffeoylarbutin solution, band I undergoes a large red shift to 370 nm, while band II experiences a blue shift to 270 nm. These shifts suggest an interaction between the compound and copper (II) ion, as neither the ligand nor the metal absorbs at these specific wavelengths.

Interestingly, the addition of mTyr to the solution does not result in a change in the maximum absorption at 328 nm, corresponding to the acyl group. However, the characteristic band for the aromatic group at 290 nm exhibits a slight blue shift to 286 nm, accompanied by an increase in intensity after incubation with mTyr. This phenomenon indicates a twist in the planar structure of 6′-*O*-caffeoylarbutin following complex formation, rather than direct chelation with the copper (II) ion located in the catalytic active center of the enzyme. The interaction of 6′-*O*-caffeoylarbutin with the aromatic group suggests its involvement in the nucleophilic attack at the active site of mTyr, resulting in the observed decrease in catalytic activity.

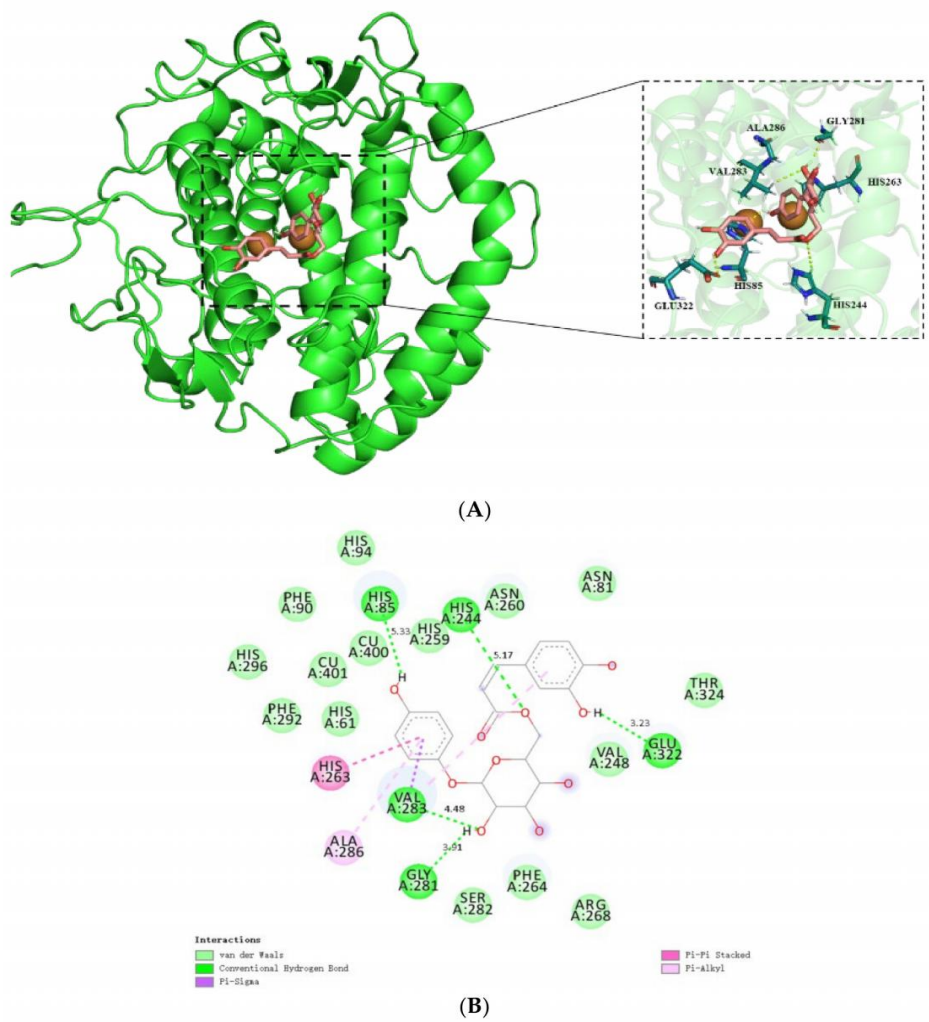

Figure 5. Molecular docking simulation of 6′-*O*-caffeoylarbutin with mTyr: (**A**). The docking of 6′-*O*-caffeoylarbutin with the pocket of mTyr. (**B**). The docking of 6′-*O*-caffeoylarbutin with amino acid residue of pocket of mTyr.

Moreover, 6′-*O*-caffeoylarbutin predominantly interacts with 15 amino acid residues through van der Waals forces. Among them, four hydrophobic residues, namely Val248, Phe90, Phe264, and Phe292, located at the periphery of the binding cavity, contribute to its hydrophobic nature. The incorporation of the caffeoyl group into beta-arbutin significantly alters the binding interactions between the protein and ligand, thereby enhancing the targeting ability of 6′-*O*-caffeoylarbutin towards mTyr. The docking results demonstrate that 6′-*O*-caffeoylarbutin induces conformational changes in the active site, impairing the functionality of the enzyme. The dominant conformation of 6′-*O*-caffeoylarbutin can be regarded as an inhibitor, as the formation of the enzyme_inhibitor complex impedes the release of oxidation products and the entry of L-DOPA. This finding provides a plausible explanation for the diphenolase inhibitory activity of 6′-*O*-caffeoylarbutin, which is consistent with the results obtained from HPLC analysis.

In summary, the UV_vis absorption spectra provide valuable insights into the interaction between 6′-*O*-caffeoylarbutin, mTyr, and copper (II) ions. The observed shifts in absorption bands and changes in intensity indicate the formation of complexes and conformational changes in 6′-*O*-caffeoylarbutin upon binding to mTyr. These findings contribute to our understanding of the inhibitory effects of 6′-*O*-caffeoylarbutin on the catalytic activity of mTyr.

2.1.4. The Fluorescence Quenching Effect of 6′-*O*-Caffeoylarbutin on mTyr

Fluorescence quenching refers to the phenomenon in which the intensity of fluorescence decreases as a result of interactions between molecules and fluorescent substances. These interactions can involve excited-state reactions, molecular rearrangements, energy transfer, formation of ground-state complexes, and collisional quenching [18,19].

In Figure 4B, curve 1 represents the fluorescence emission spectrum of mTyr. The intrinsic fluorescence of mTyr primarily originates from tyrosine residues at 320 nm and tryptophan residues at 335 nm. Binding of small molecules to mTyr induces changes in the microenvironment of the amino acid residues, resulting in alterations in the fluorescence intensity [20]. Curve 10 corresponds to the fluorescence emission spectrum of 6′-*O*-caffeoylarbutin, while curves 2–9 represent the fluorescence emission spectra of 6′-*O*-caffeoylarbutin at concentrations of 5, 10, 15, 25, 50, 75, 90, and 100 μM, respectively.

The results demonstrate a significant decrease in the fluorescence intensity of mTyr in the presence of 6′-*O*-caffeoylarbutin, indicating the quenching of the intrinsic fluorescence of mTyr. Moreover, the fluorescence intensity shows a concentration-dependent reduction. As observed in Figure 4B, with increasing concentrations of 6′-*O*-caffeoylarbutin, the fluorescence intensity of mTyr gradually decreases. At a concentration of 25 μM 6′-*O*-caffeoylarbutin, the peak of the fluorescence emission spectrum of mTyr experiences a reduction of 37.18% (Figure S5A). Further increasing the concentration to 100 μM results in a decrease of 12.57% in the fluorescence emission spectrum of mTyr. These findings suggest that 6′-*O*-caffeoylarbutin induces quenching of the intrinsic fluorescence of mTyr, indicating a potential interaction between 6′-*O*-caffeoylarbutin and mTyr.

According to Kim et al. [21], hydroxyl groups in inhibitors primarily contribute to quenching the intrinsic fluorescence of enzymes. Therefore, it can be inferred that 6′-*O*-caffeoylarbutin predominantly quenches the fluorescence of mTyr by interacting with the hydroxyl group on its phenyl ring.

Additionally, as the concentration of 6′-*O*-caffeoylarbutin increases, the emission peak of tryptophan residues in tyrosinase shifts from 335 nm to 355 nm, indicating a significant redshift. Similarly, the emission peak of tyrosine residues at 320 nm shifts to 310 nm, demonstrating a noticeable blueshift. This phenomenon may be attributed to the relatively hydrophobic nature of the tryptophan and tyrosine amino acid residues in mTyr. The fluorescence spectra of these residues are sensitive to changes in the surrounding microenvironment. Studies have shown that a blue shift in the emission spectrum suggests alterations in the microenvironment near tryptophan residues, while a red shift corresponds to changes in the microenvironment near tyrosine residues [22]. Therefore, it can be inferred that an interaction occurs between mTyr and 6′-*O*-caffeoylarbutin, resulting in a decrease in polarity around the tryptophan residues in mTyr, leading to a more hydrophobic environment [23]. These observations indicate that the interaction between 6′-*O*-caffeoylarbutin and mTyr induces conformational changes in the enzyme.

Fluorescence quenching can be classified into static quenching and dynamic quenching. Static quenching occurs when quenching agents bind to fluorescent substances, forming complexes that result in quenching. Dynamic quenching, on the other hand, primarily arises from thermal motion and molecular collisions. In this study, the quenching results were analyzed using the Stern_Volmer equation, as shown in Figure S5B. The plot of F0/F against the concentration of 6′-*O*-caffeoylarbutin yielded a straight line with a good linear relationship ($R^2 = 0.9802$). The slope of this line can be used to calculate the quenching rate constant Kq, which was determined to be 4.11×10^{12} L·(mol·s)$^{-1}$. Typically, the thresh-

International Journal of
Molecular Sciences

MDPI

Article

6′-*O*-Caffeoylarbutin from Quezui Tea: A Highly Effective and Safe Tyrosinase Inhibitor

Dong Xie [1,†], Wengan Fu [1,†], Tiantian Yuan [1], Kangjia Han [1], Yuxiu Lv [1], Qi Wang [1], Qian Jiang [1], Yingjun Zhang [2], Guolei Zhu [1], Junming Xu [3], Ping Zhao [1,*] and Xiaoqin Yang [1,*]

[1] Laboratory of National Forestry and Grassland Administration on Highly-Efficient Utilization of Forestry Biomass Resources in Southwest China, Southwest Forestry University, Kunming 650224, China; dong-xie@outlook.com (D.X.); 18751856651@163.com (W.F.); 19387322404@163.com (T.Y.); xqyhankangjia6174@163.com (K.H.); lvyuxiu0130@outlook.com (Y.L.); qiwang202312@163.com (Q.W.); m17368708632@163.com (Q.J.); guoleizhu@163.com (G.Z.)
[2] Laboratory of Phytochemistry and Plant Resources in West China, Kunming Institute of Botany, Chinese Academy of Sciences, Kunming 650204, China; zhangyj@mail.kib.ac.cn
[3] Institute of Chemical Industry of Forest Products, Chinese Academy of Forestry, Nanjing 210042, China; xujunming@icifp.cn
* Correspondence: hypzhao2022@163.com (P.Z.); yangxiaoqin@swfu.edu.cn (X.Y.)
† These authors contributed equally to this work.

Abstract: Tyrosinase is vital in fruit and vegetable browning and melanin synthesis, crucial for food preservation and pharmaceuticals. We investigated 6′-*O*-caffeoylarbutin's inhibition, safety, and preservation on tyrosinase. Using HPLC, we analyzed its effect on mushroom tyrosinase and confirmed reversible competitive inhibition. UV_vis and fluorescence spectroscopy revealed a stable complex formation with specific binding, causing enzyme conformational changes. Molecular docking and simulations highlighted strong binding, enabled by hydrogen bonds and hydrophobic interactions. Cellular tests showed growth reduction of A375 cells with mild HaCaT cell toxicity, indicating favorable safety. Animal experiments demonstrated slight toxicity within safe doses. Preservation trials on apple juice showcased 6′-*O*-caffeoylarbutin's potential in reducing browning. In essence, this study reveals intricate mechanisms and applications of 6′-*O*-caffeoylarbutin as an effective tyrosinase inhibitor, emphasizing its importance in food preservation and pharmaceuticals. Our research enhances understanding in this field, laying a solid foundation for future exploration.

Keywords: 6′-*O*-caffeoylarbutin; tyrosinase inhibitor; inhibitory mechanism; computational simulation; food preservation

Citation: Xie, D.; Fu, W.; Yuan, T.; Han, K.; Lv, Y.; Wang, Q.; Jiang, Q.; Zhang, Y.; Zhu, G.; Xu, J.; et al. 6′-*O*-Caffeoylarbutin from Quezui Tea: A Highly Effective and Safe Tyrosinase Inhibitor. *Int. J. Mol. Sci.* **2024**, *25*, 972. https://doi.org/10.3390/ijms25020972

Academic Editor: Davide Barreca

Received: 14 November 2023
Revised: 11 December 2023
Accepted: 15 December 2023
Published: 12 January 2024

1. Introduction

Tyrosinase (EC 1.14.18.1), also referred to as polyphenol oxidase, is widely distributed across plants, animals, and microorganisms [1,2]. Illustrated in Figure S1, tyrosinase functions as a pivotal, rate-limiting, multifunctional copper (II)-containing metalloenzyme that plays a crucial role in melanin biosynthesis [3]. The primary biochemical functions of tyrosinase encompass the hydroxylation of L-tyrosine into L-dihydroxyphenylalanine (L-DOPA), followed by the subsequent oxidation of L-DOPA leading to the formation of DOPA-quinone. Additionally, tyrosinase has the potential to facilitate the oxidation of 5,6-dihydroxyindole, resulting in the production of indole-5,6-quinone [4]. In plants, tyrosinase orchestrates the conversion of phenolic compounds into quinone substances. Subsequent polymerization of these quinones generates pigments accountable for the occurrence of browning phenomena [5]. This process directly impacts the inherent visual appeal and nutritional value of various foods like fruits, juices, and vegetables, consequently diminishing their market value. Hence, the inhibition of tyrosinase activity and interception of the DOPA oxidation pathway have emerged as robust strategies in notably curbing melanin production, particularly in contexts that involve counteracting the browning processes.